Search for memory and return to disorder in potassium-lithium tantalate crystals

2000 J. Phys.: Condens. Matter 12 1461

(http://iopscience.iop.org/0953-8984/12/7/327)

J. Phys.: Condens. Matter **12** (2000) 1461–1471. Printed in the UK PII: S0953-8984(00)08611-2

Search for memory and return to disorder in potassium–lithium tantalate crystals

P Doussineau†, T de Lacerda-Arôso‡ and A Levelut†

† Laboratoire des Milieux Désordonnés et Hétérogènes§, Université P et M Curie, Case 86, 75252 Paris Cédex 05, France

‡ Departamento de Fisica, Universidade do Minho, 4709 Braga, Portugal

Received 11 October 1999 , in final form 10 December 1999

Abstract. Return to disorder, and less frequently memory, have been demonstrated in various disordered materials. In order to find the conditions necessary for the observation of these effects, the evolution of the real part ε' of the dielectric constant of two disordered paraelectric crystals $K_{1-x}Li_xTaO_3$ (KLT) has been extensively studied by the means of the capacitance $C(T, t)$ around the beginning and the end of a temperature plateau. The return to disorder and memory effects have not been seen in KTL, in contrast to what was recently observed in disordered ferroelectric crystals $KTa_{1-y}Nb_yO_3$ of a similar family. The variations $dC = P(T_0, t_0)\,dT + Q(T_0, t_0)\,dt$ in the vicinity of the point (T_0, t_0) are split into a contribution depending on temperature only and an isothermal contribution only depending on time. All the results of such an analysis of the features observed in KLT can be explained by the domain wall model in its original form.

1. Introduction

Ageing is a phenomenon currently observed in many materials such as spin glasses, polymers, structural glasses and so on. It seems that a necessary condition for its occurrence is disorder and frustration. Ageing manifests itself by the slow evolution, depending on the history of the sample, of some characteristics of the material. Examples of such time-dependent characteristics are the complex magnetic susceptibility χ of spin glasses (SGs) [1–3], the static elastic compliance s of polymers [4] and the complex dielectric constant ε of disordered dielectrics [5, 6]. In this last case, potassium–lithium tantalate $K_{1-x}Li_xTaO_3$ (KLT) and potassium niobo-tantalate $KTa_{1-y}Nb_yO_3$ (KTN) crystals have been extensively studied.

The comparison between the time-dependent properties of these two families of materials is of the highest interest. Indeed, at low temperatures where the experiments are usually performed, the KLT crystals are in the paraelectric phase while the KTN crystals are in the ferroelectric phase. Does this difference induce different ageing properties?

A first answer is given by experiments on ergodicity breaking. If the phase space of a system is split into several mutually inaccessible regions, the system may arrive at several different equilibrium states according to the initial state where it is initially left. This is true ergodicity breaking [7]. Phase transitions provide examples of such splittings. However, it may happen that equilibrium is unique but the time necessary to travel from the initial state to the equilibrium state is infinite for fundamental reasons. This is weak ergodicity breaking [8].

§ Associated with the Centre National de la Recherche Scientifique (UMR 7603).

0953-8984/00/071461+11$30.00

Indeed, these two cases correspond to purely theoretical situations. In real materials, neither the height of energy barriers in the phase space nor the number of traps are infinite.

Practically, for experimentalists, it is often difficult to assert if a long evolution (lasting one year, for instance) is finite or infinite. Moreover, if the sample is imposed to start from different initial states and is observed to arrive after a long time to different states, it is difficult to decide if it would finally have reached a unique equilibrium state or not after a longer time. Indeed, such an ambiguous situation (even complemented by numerical extrapolations) leaves open the question of ergodicity or non-ergodicity. This is called effective ergodicity breaking. From dielectric measurements it was found that both KLT crystals and KTN crystals showed effective ergodicity breaking [6]. From this result we infer that the effect is not related to paraelectricity or ferroelectricity. Finally, we notice that effective ergodicity breaking is an experimental concept not incompatible with ergodicity (as paraelectrics must show); it is only a question of time or patience.

In order to explain the KLT behaviour a model was proposed [9]. According to this model, the time-dependent part $\delta\varepsilon(\omega, t)$ of the alternative dielectric constant is attributed to the wall motion of polarization domains growing in the tantalate lattice.

In a pure paraelectric compound, the polarization is an essentially fluctuating quantity, which varies rapidly and permanently in time and space. It is only in the vicinity of the para–ferroelectric phase transition that the movements of the polarized regions become slower (critical slowing down). In the same time the size of these regions, called the coherence length $\xi(T)$ of the polarization fluctuations, becomes larger and eventually diverges at the critical point.

In contrast to the case of pure crystals, compounds such as KLT crystals contain a high density of impurities acting as sources of static random fields at low temperatures. These static fields hinder the flips of the lattice dipoles. As a consequence we may assume that, instead of polarization fluctuations vanishing on a microscopic time scale, any deviation of the polarization out of the equilibrium value (zero in this case) has a very long relaxation time. In other words, the motion of the polarized regions turns out to be noticeable only after a duration of the order of thousands of seconds because the wall which separates two such regions is pinned near lattice sites occupied by polar impurities. Of course, the size of these regions is limited by the temperature dependent coherence length $\xi(T)$. A polarized region with such a long lifetime is not essentially different from what is usually called a domain in a ferroelectric phase. In this latter case the polarization domains are in principle infinite. However, when their growth is hindered by static random fields their dynamics becomes very slow and their size remains finite just as in the paraelectric case. In both cases when $\delta\varepsilon(\omega, t)$ is measured the time evolution due to the slow motion of walls appears as quasi-static on the time scale of the oscillating electric field. Moreover, the effect on the dielectric constant is proportional to the total wall area. When the domain size ρ increases towards $\xi(T)$ the individual area increases as ρ^2. The number of domains is proportional to ρ^{-3} and consequently the total area decreases as ρ^{-1}. This is the expected behaviour. The assumption of proportionality of $\delta\varepsilon$ to the total wall area is probably not true (the response of an elementary area depends on its angle with the oscillating electric field) but this is not important if the domain growth follows a scaling law (during the evolution, all the lengths are multiplied by the same number).

Finally, in what follows we use the word domain in the extended meaning of very slowly varying polarized regions in the paraelectric phase and their frontier, even if it is fuzzy, is called a domain wall.

Recently, two unusual effects were observed in the ferroelectric phase of KTN crystals [10]. A regular cooling at the rate $\mathrm{d}T/\mathrm{d}t = -r$ is interrupted by an isothermal evolution or plateau at the temperature T_{pl}. At this temperature ageing manifests itself by the decrease of

the real ε' and imaginary ε'' parts of the dielectric constant $\varepsilon = \varepsilon' - \mathrm{i}\varepsilon''$. This evolution tends necessarily towards more stability and thus more order. If cooling is then resumed at the same constant rate $-r$, the two parts ε' and ε'' first increase, thus indicating some return to disorder (although the temperature is lowered). This is the first effect. If cooling is carried on down to low temperatures and followed by a steady heating at the opposite rate $+r$, minima of ε' and ε'' are observed when passing back through the temperature T_{pl} . This means that the sample has kept some memory of the hole which was dug in the dielectric constant by ageing at this temperature. This permanent memory can be erased by annealing. This is the second effect. We emphasize that memory does not mean that some signal has not yet achieved its monotonic relaxation towards fading. In fact, it is an effect localized in temperature (around T_{pl}) which is nonmonotonic in time when the temperature is regularly increased.

The three effects (ageing, return to disorder, memory) just mentioned deserve more comments. Ageing is very frequently observed in disordered materials [1–6]. Return to disorder is rather frequent: it was observed in a wide range of cases such as the ferroelectric lock-in phase of Rb_2ZnCl_4 [11], in the SG phase of $CdCr_{1.7}In_{0.3}S_4$ [12], in KTN [10], in Plexiglass (PMMA) [13] and in both phases (SG and ferromagnetic) of $CdCr_{1.9}In_{0.1}S_4$ [14]. Memory is less frequent: it exists in the modulated phase of thiourea [15] and in Plexiglass but not in Rb_2ZnCl_4; it is present in the SG phase of $CdCr_{1.9}In_{0.1}S_4$ but not in its ferromagnetic phase; it is clearly seen in the ferroelectric phase of KTN.

Obviously, a rule is missing which would allow us to predict whether a disordered material will show return to disorder and memory or not. In this context the study of the KLT series may be very helpful because many results about ageing in these materials are already available and because these crystals belong to a family close parent of the KTN series which presents the memory effect.

In the present article we report on an extensive study of the evolution of the dielectric constant after a plateau and on a search for memory and return to disorder in KLT. Our main point is that we have found no trace of memory and return to disorder, but we have checked that our results are well described by the domain model in its original form.

2. Experiments

The pure potassium tantalate $KTaO_3$ crystal is a cubic perovskite. It is an incipient ferroelectric: the ferroelectric transition it would undergo at 0 K is aborted, due to quantum fluctuations. However, the real part ε' of the dielectric constant strongly rises as the temperature is lowered since the correlations between the displacements of the tantalate ions increase. The random substitution of Li^+ ions for K^+ ions in a $KTaO_3$ crystal has two consequences. Firstly, the Li^+ ions take off-centre positions and generate electric dipoles at random sites. The subsequent random interactions induce the freezing of the dipoles below some transition temperature T_{tr} if the Li^+ concentration x in the crystal $K_{1-x}Li_xTaO_3$ is larger than 0.01 [16–18]. Secondly, the trend of the tantalate lattice towards ferroelectricity is attenuated but the real part ε' of its dielectric constant is still increasing when the temperature decreases. This is the signature of growing domains of fluctuating polarization. The slow dynamics and ageing observed in KLT are attributed to the motion, hindered by the static random fields generated by the frozen Li^+ ions, of the walls of these polarization domains of the tantalate lattice [9].

Using a Hewlett–Packard 4192A impedance analyser, we have measured the electric capacitance at seven frequencies, ranging from 1 kHz to 1 MHz. It can easily be transformed into the real part ε' of the complex dielectric constant. In KLT the dielectric loss is very weak and the imaginary part ε'' is unusable. The dielectric constant $\varepsilon(\omega, t)$ was measured as a function of time while the sample temperature $T(t)$ was a controlled function of time.

In KLT the freezing temperature T_{tr} of the dipoles is related to the lithium concentration x by the law $T_{tr}(x) = 535x^{2/3}$ [19]. The curve $T_{tr}(x)$ separates the paraelectric region and the glassy region in the phase diagram. For the experiments reported here, two samples with lithium concentrations $x = 0.017\,(T_{tr} = 34\ K)$ and $x - 0.025\,(T_{tr} = 45\ K)$ were used. In the former, since the lithium concentration is lower, ferroelectricity is less hindered and the dielectric constant (and the capacitance) is much larger than in the latter at low temperatures. The typical sizes of the samples were $4 \times 4 \times 6$ mm^3. Chromium electrodes were deposited on the largest faces.

All our experiments begin by an annealing near 50 K and an initial rapid cooling across the transition temperature T_{tr} down to $T_{max} \cong 20$ K. Then several procedures were used. They were composed of a cooling at a constant rate $\mathrm{d}T/\mathrm{d}t = -r$, a heating at the opposite rate $\mathrm{d}T/\mathrm{d}t = +r$ and a temperature plateau T_{pl}. These three components were combined in different manners explained in detail in subsection 3.2. Three temperatures play particular roles: the minimum temperature $T_{min} \cong 4.8$ K (slightly above the liquid helium temperature), T_{pl} and T_{max}. The curves recorded at different measuring frequencies are similar. Consequently, we only present our data at 100 kHz. The measurements are generally performed at the rate of one point every 19 s with the temperature change equal either to 0 (plateau) or to ± 0.06 K; this gives heating and cooling rates with $r = 0.0032$ K s^{-1}. The steps are small enough to draw quasi-continuous curves and to deduce the slopes needed for our analysis.

3. Analysis of the data

3.1. Method

We have studied differential variations of the capacitance $C(T, t)$ in the vicinity of several remarkable points (T_0, t_0) in the (T, t) space. Taking $C(T_0, t_0)$ as reference, the deviation from this value is $\mathrm{d}C = C(T_0 + \mathrm{d}T, t_0 + \mathrm{d}t) - C(T_0, t_0)$. For infinitesimal changes, we assume that $\mathrm{d}C$ is the sum of an instantaneous change proportional to $\mathrm{d}T$ and of a decrease due to ageing, proportional to $\mathrm{d}t$. This reads

$$\mathrm{d}C = P(T_0, t_0)\,\mathrm{d}T + Q(T_0, t_0)\,\mathrm{d}t. \tag{1}$$

The coefficients $P(T_0, t_0)$ and $Q(T_0, t_0)$ are the partial derivatives of $C(T, t)$ with respect to T and t. They are related to the slopes of the curves of $C(T, t)$ in the vicinity of (T_0, t_0). The coefficient P depends on temperature and possibly on time; it is negative for a paraelectric material such as KLT. The coefficient Q is generally negative and it depends on temperature. Its absolute value obviously decreases with time: isothermal ageing becomes slower and slower.

The two coefficients P and Q of equation (1) can generally be determined by two paths in the (T, t) space between the point (T_0, t_0) and two other different points $(T_0 + \mathrm{d}T, t_0 + \mathrm{d}t)$. If one or two other paths are available, they provide an independent determination of one or two of these coefficients. This is a check of our assumptions.

The constant derivative $r = \mathrm{d}T/\mathrm{d}t$ is the temperature change rate. It is written r_c for cooling ($r_c < 0$) or r_h for heating ($r_h > 0$); in our experiments $r_c = -r_h$ and, obviously $r = 0$ during the plateau. Since in our experiments $\mathrm{d}T$ and $\mathrm{d}t$ are proportional we put $\tilde{Q}(T_0, t_0) = Q(T_0, t_0)/|r|$, and hereafter we conventionally measure the isothermal variations and the isochronous variations with the same units (in pF K^{-1}). On the same footing, we can write $\hat{P}(T_0, t_0) = P(T_0, t_0) + \tilde{Q}(T_0, t_0)$, the effective (or total) derivative $\hat{P}$ of C with respect to T.

We take as time origin the instant when the plateau temperature T_{pl} is reached. Therefore, the beginning of the plateau corresponds to $t_0 = 0$ and the end to $t_0 = t_{pl}$, with $t_{pl} = 10\,000$ s. The plateau temperature is $T_{pl} = 11.15$ K.

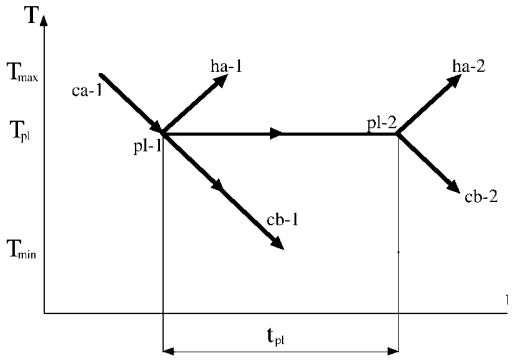

Figure 1. Schematic representation of the four thermal histories used in our experiments. The different procedures are:

(i) path ca-1 + path ha-1: cooling from $T_{max} \cong 20$ K down $T_{pl} = 11.15$ K and subsequent heating from T_{pl} up to T_{max};
(ii) path ca-1 + plateau at T_{pl} + path ha-2: cooling from T_{max} down T_{pl}, isotherm and heating from T_{pl} up to T_{max};
(iii) path ca-1 + path cb-1: cooling from T_{max} down to $T_{min} \cong 4.8$ K;
(iv) path ca-1 + plateau at T_{pl} + path cb-2: cooling from T_{max} down to T_{pl}, isotherm and cooling from T_{pl} down to T_{min}.

The different paths in the (T, t) space are referred according to the following notation. The points $(T_{pl}, 0)$ and (T_{pl}, t_{pl}) are respectively called points 1 and 2. The letters c and h mean cooling and heating while the letters a and b mean above and below, respectively. An isothermal path is labelled by pl. Hence, for instance, path ca-1 leads to point 1 by cooling from above while path pl-2 arrives at point 2 along the plateau. The possible paths passing through points 1 and/or 2 are drawn in figure 1.

The four different procedures used were the following sequences:

(i) cooling from T_{max} to T_{pl} (path ca-1) + heating from T_{pl} to T_{max} (path ha-1);
(ii) cooling from T_{max} to T_{pl} (path ca-1) + plateau at T_{pl} + heating from T_{pl} to T_{max} (path ha-2);
(iii) cooling from T_{max} to T_{min} (path ca-1 + path cb-1) + heating from T_{min} to T_{max};
(iv) cooling from T_{max} to T_{pl} (path ca-1) + plateau at T_{pl} + cooling from T_{pl} to T_{min} (path cb-2) + heating from T_{min} to T_{max}.

In the following study we focus our attention around points 1 and 2 in the (T, t) space.

3.2. On the plateau

We have first examined the isothermal ($r = 0$) variation of $C(T, t)$. An example is displayed in figure 2 which clearly shows that the capacitance decay becomes slower and slower. The measurements have been made in the vicinity of its beginning and of its end. The corresponding paths pl-1 and pl-2 in the (T, t) space are

$$(T_{pl}, 0) \rightarrow (T_{pl}, \delta t) \quad \text{and} \quad (T_{pl}, t_{pl} - \delta t) \rightarrow (T_{pl}, t_{pl})$$

and the capacitance deviations are respectively

$$\mathrm{d}C_{pl\text{-}1} = C(T_{pl}, \delta t) - C(T_{pl}, 0) = Q(T_{pl}, 0)\delta t < 0 \tag{2}$$

and

$$\mathrm{d}C_{pl\text{-}2} = C(T_{pl}, t_{pl} - \delta t) - C(T_{pl}, t_{pl}) = -Q(T_{pl}, t_{pl})\delta t > 0. \tag{3}$$

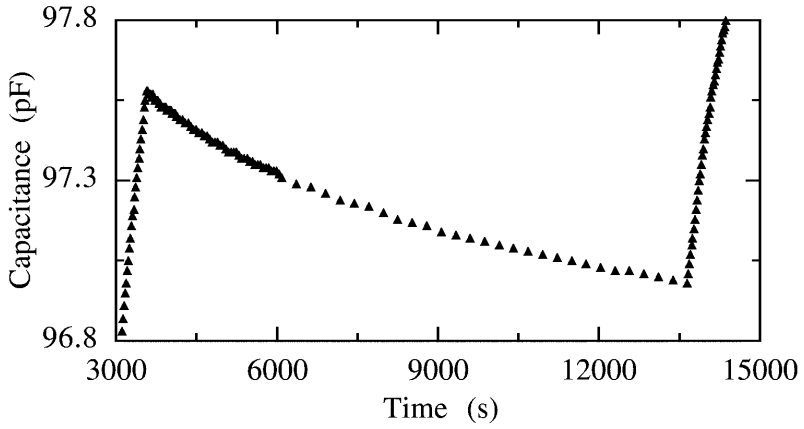

Figure 2. Isothermal decay (lasting 10 000 s) of the real part of the capacitance recorded at 100 kHz in a $K_{1-x}Li_xTaO_3$ sample with $x = 0.017$. The displayed data are a part of procedure (iv), cooling from T_{max} down to T_{pl}, isotherm and cooling from T_{pl} down to T_{min}.

We have measured for the sample with $x = 0.017$ concentration

$$\tilde{Q}(T_{pl}, 0) = -(0.050 \pm 0.003) \text{ pF K}^{-1} \quad \text{and} \quad \tilde{Q}(T_{pl}, t_{pl}) = -(0.011 \pm 0.0015) \text{ pF K}^{-1}$$

and for the one with $x = 0.025$ concentration

$$\tilde{Q}(T_{pl}, 0) = -(0.025 \pm 0.003) \text{ pF K}^{-1} \quad \text{and} \quad \tilde{Q}(T_{pl}, t_{pl}) = -(0.005 \pm 0.001) \text{ pF K}^{-1}.$$

3.3. Above the plateau temperature

Now we examine the paths ca-1, ha-1 and ha-2 which are above T_{pl}.

On the one hand, we have

$$\text{path ca-1} \qquad (T_{pl} + \delta T, -\delta t) \rightarrow (T_{pl}, 0) \qquad (r = r_c)$$
$$\text{path ha-1} \qquad (T_{pl}, 0) \rightarrow (T_{pl} + \delta T, \delta t) \qquad (r = r_h).$$

The corresponding capacitance changes are

$$\mathrm{d}C_{ca\text{-}1} = C(T_{pl} + \delta T, -\delta t) - C(T_{pl}, 0) = P(T_{pl}, 0)\delta T - Q(T_{pl}, 0)\delta t \tag{4}$$
$$\mathrm{d}C_{ha\text{-}1} = C(T_{pl} + \delta T, \delta t) - C(T_{pl}, 0) = P(T_{pl}, 0)\delta T + Q(T_{pl}, 0)\delta t. \tag{5}$$

In the $x = 0.017$ concentration sample the following values were obtained

$$P(T_{pl}, 0) = -(0.545 \pm 0.005) \text{ pF K}^{-1} \quad \text{and} \quad \tilde{Q}(T_{pl}, 0) = -(0.050 \pm 0.005) \text{ pF K}^{-1}$$

and for the sample with $x = 0.025$ concentration

$$P(T_{pl}, 0) = -(0.225 \pm 0.005) \text{ pF K}^{-1} \quad \text{and} \quad \tilde{Q}(T_{pl}, 0) = -(0.025 \pm 0.005) \text{ pF K}^{-1}.$$

We notice that the values obtained here for $\tilde{Q}(T_{pl}, 0)$ are in very good agreement with those previously obtained along the plateau.

On the other hand, there is

$$\text{path ha-2} \qquad (T_{pl}, t_{pl}) \rightarrow (T_{pl} + \delta T, t_{pl} + \delta t) \qquad (r = r_h).$$

The corresponding capacitance change is

$$\mathrm{d}C_{ha\text{-}2} = C(T_{pl} + \delta T, t_{pl} + \delta t) - C(T_{pl}, t_{pl}) = P(T_{pl}, t_{pl})\delta T + Q(T_{pl}, t_{pl})\delta t. \tag{6}$$

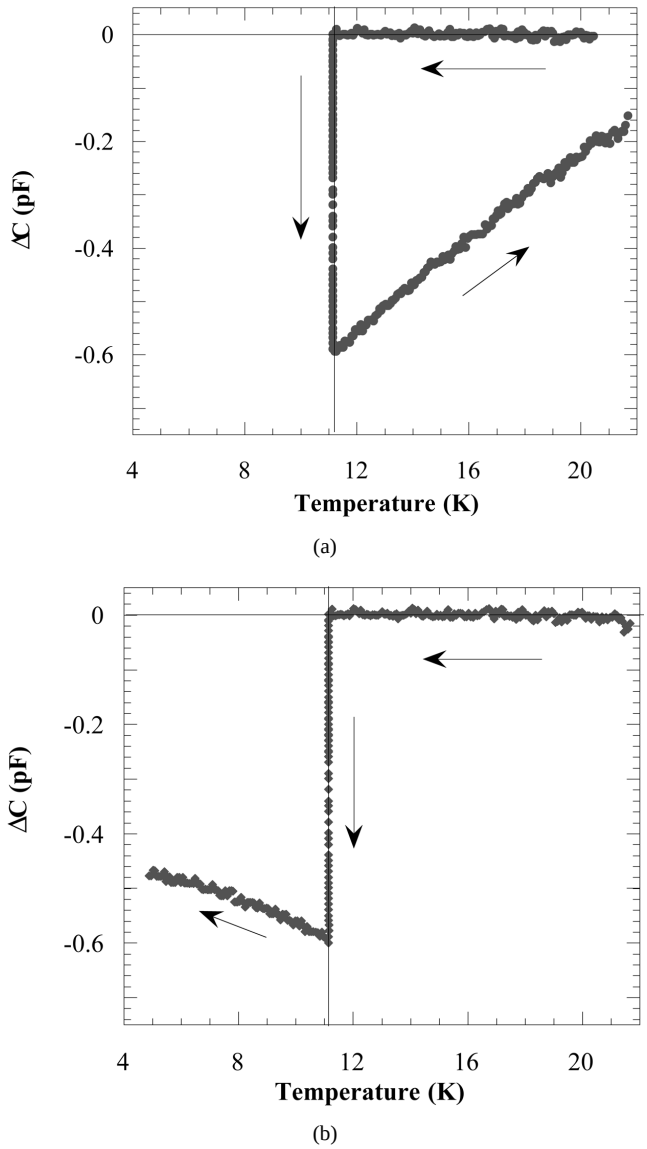

Figure 3. Difference between the real parts of the capacitances of a $K_{1-x}Li_xTaO_3$ sample and their appropriate references, shown as a function of the temperature. Data has been recorded at 100 kHz in a ($x = 0.017$) sample during the following two thermal sequences.

(a) Cooling from $T_{max} \cong 20$ K down to $T_{pl} = 11.15$ K, isotherm for 10 000 s and heating from T_{pl} up to T_{max}. Reference: path ca-1 + path ha-1.
(b) Cooling from T_{max} down to T_{pl}, isotherm and cooling from T_{pl} down to T_{min}. Reference: path ca-1 + path cb-1.

The only difference between the thermal histories of paths ha-1 and ha-2 is the plateau. With the values previously found for $\tilde{Q}(T_{pl}, t_{pl})$, we obtain for the $x = 0.017$ concentration sample

$$P(T_{pl}, t_{pl}) = -(0.55 \pm 0.01) \text{ pF K}^{-1}$$

and for the one with $x = 0.025$ concentration

$$P(T_{pl}, t_{pl}) = -(0.25 \pm 0.01) \text{ pF K}^{-1}.$$

The comparison with our preceding results show that $P(T_{pl}, t_{pl}) = P(T_{pl}, 0)$, within experimental accuracy. We conclude that the coefficient $P(T_{pl})$ does not depend on time. Consequently, the difference of slopes between the paths ha-1 and ha-2 must be

$$\hat{P}(T_{pl}, t_{pl}) - \hat{P}(T_{pl}, 0) \cong -0.04 \text{ pF K}^{-1}$$
$$\hat{P}(T_{pl}, t_{pl}) - \hat{P}(T_{pl}, 0) \cong -0.02 \text{ pF K}^{-1}$$

for $x = 0.017$ and $x = 0.025$ samples, respectively. This is confirmed by figure 3(a) where we find (0.045 ± 0.005) pF K^{-1} for the first sample. This is a check of the coherence of our method.

This result, valid for the initial slopes just above T_{pl}, also explains why the two curves relative to the paths ha-1 and ha-2 tend to merge together: along the path ha-1 the system is young (the domains are rather small and therefore able to grow rapidly) while along the path ha-2 the system is old (the domains have grown during the plateau and their motions have become slow).

3.4. Below the plateau temperature

Now we examine the paths cb-1 and cb-2 which are below T_{pl}. The plateau is the only difference between their thermal histories. They are

path cb-1 $\quad (T_{pl}, 0) \rightarrow (T_{pl} - \delta T, \delta t) \qquad (r = r_c)$
path cb-2 $\quad (T_{pl}, t_{pl}) \rightarrow (T_{pl} - \delta T, t_{pl} + \delta t) \qquad (r = r_c).$

The corresponding capacitance changes are

$$\mathrm{d}C_{cb\text{-}1} = C(T_{pl} - \delta T, \delta t) - C(T_{pl}, 0) = -P(T_{pl}, 0)\,\delta T + Q(T_{pl}, 0)\,\delta t \tag{7}$$
$$\mathrm{d}C_{cb\text{-}2} = C(T_{pl} - \delta T, t_{pl} + \delta t) - C(T_{pl}, t_{pl}) = -P(T_{pl}, t_{pl})\,\delta T + Q(T_{pl}, t_{pl})\,\delta t. \tag{8}$$

From the preceding results we are able to predict that the effective slopes must be

$$\hat{P}(T_{pl}, 0) = -(0.495 \pm 0.01) \text{ pF K}^{-1} \quad \text{and} \quad \hat{P}(T_{pl}, t_{pl}) = -(0.535 \pm 0.01) \text{ pF K}^{-1}$$
$$\hat{P}(T_{pl}, 0) = -(0.23 \pm 0.01) \text{ pF K}^{-1} \quad \text{and} \quad \hat{P}(T_{pl}, t_{pl}) = -(0.25 \pm 0.01) \text{ pF K}^{-1}$$

for the two samples.

Moreover, the difference of slopes between the paths cb-1 and cb-2 must be

$$\hat{P}(T_{pl}, t_{pl}) - \hat{P}(T_{pl}, 0) \cong -0.04 \text{ pF K}^{-1}$$
$$\hat{P}(T_{pl}, t_{pl}) - \hat{P}(T_{pl}, 0) \cong -0.02 \text{ pF K}^{-1}$$

for the samples with $x = 0.017$ and $x = 0.025$, respectively. This is confirmed by figure 3(b) where we find (0.037 ± 0.005) pF K^{-1} for the first sample. This is another check of the coherence of our method.

Here too, this result, valid for the initial slopes just below T_{pl}, also explains why the two curves relative to the paths cb-1 and cb-2 tend to be parallel: when the temperature decreases the ageing process steadily slows down and the difference of ageing velocity between a young system (without any plateau) and an old system (after the plateau) becomes weaker and weaker and finally vanishes.

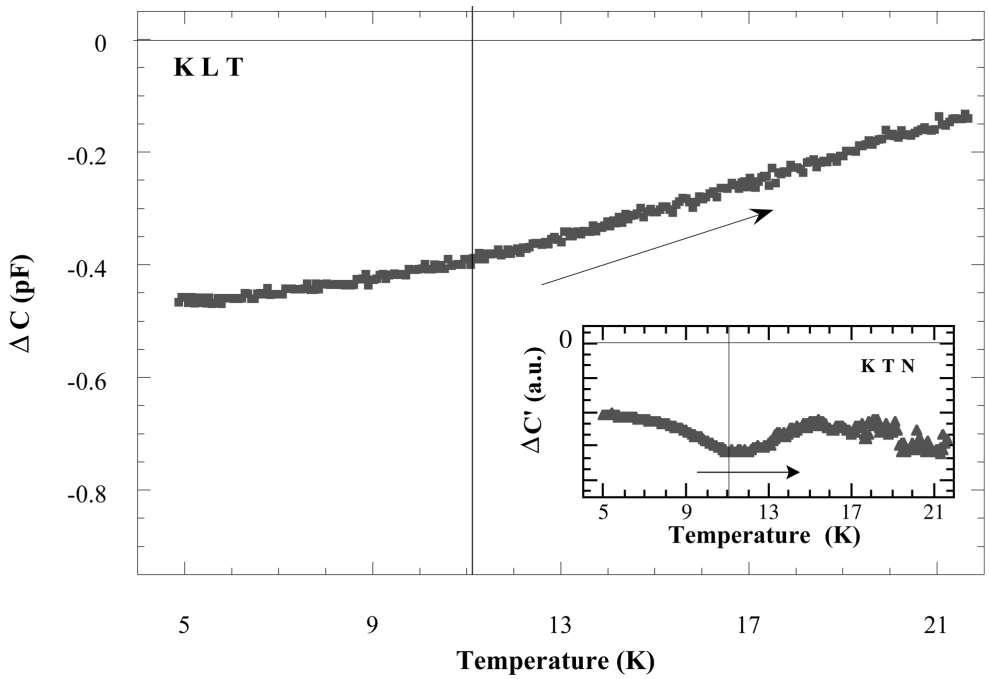

Figure 4. Difference between two real parts of $K_{1-x}Li_xTaO_3$ ($x = 0.017$) capacitance, both recorded during heating from T_{min} up to T_{max} at 100 kHz, shown as a function of temperature. In one of the procedures, taken as reference, the sample is cooled from T_{max} down to T_{min} at constant rate. In the other one, the sample is first cooled from T_{max} down to T_{pl} at the same rate, then isothermally evolves at T_{pl} for 10 000 s and finally is cooled down to T_{min}. In the inset the same quantity is shown for $KTa_{1-y}Nb_yO_3$ ($y = 0.027$) obtained under similar conditions.

3.5. From T_{min} to T_{max}

Figure 4 shows, as a function of temperature, the difference between two curves both recorded during heating from T_{min} to T_{max}. One followed a cooling interrupted by a plateau at T_{pl} while the other, taken as reference, followed a regular cooling (without plateau) from T_{max} to T_{min}. The difference monotonically increases from a negative value due to ageing at T_{pl} and tends towards 0 near transition temperature T_{tr}. This monotonic behaviour is clearly in contrast with that observed for KTN [10] (see inset in figure 4) where a dip near T_{pl} indicated the memory of ageing occurred during the plateau. There is no such memory in KLT.

4. Discussion

Memory and return to disorder which have been observed in many materials, and in particular in KTN, do not appear in KLT. One could infer that the difference of behaviours of these two materials probably lies in the nature of the low temperature phases which are paraelectric (disordered) for KLT and ferroelectric (ordered) for KTN. Unfortunately, this simple idea is probably wrong, as shown by the experiments on $CdCr_{1.9}In_{0.1}S_4$ where the scheme is inverted since memory is present in the SG (disordered) phase but not in the ferromagnetic (ordered) phase. Therefore, the best we can do is to add our (negative) result to the list displayed in section 1.

Besides that, we have done an extensive study of the evolution of the dielectric constant of KLT after controlled cooling to a given temperature, followed or not by a plateau at this temperature, and the subsequent cooling or heating. Two main results were obtained.

The first point is the coherence of the whole set of our results which validates the proposed splitting of the evolution of the KLT into two independent parts defined in equation (1). The first component (proportional to P) is a function of the temperature and is found to be quasi-independent of time and possibly independent of the cooling rate. The second component (proportional to Q) is a decreasing function of time.

The second point is a new argument in favour of the model which has recently been proposed [9]. In this model the time evolution of the dielectric constant is attributed to the slow movement of polarization domain walls, hindered by static random fields (SRFs) generated by the frozen Li^+ ions. The set of SRFs which slows down the growth of a domain may be represented by an equivalent barrier height that the domain wall has to jump over. Due to the randomness of the Li^+ sites, there is a broad barrier distribution. Three types of domains can be distinguished, according to their behaviour after a perturbation: (i) the very fast domains (with low barriers) which respond immediately; (ii) the very slow domains (with high barriers) which are not able to respond; (iii) the intermediate domains (with intermediate barriers) which are able to follow (more or less) the perturbation. Obviously, these dividing lines are relative to a given temperature and to some characteristic experimental time (the duration of an experiment, for instance). Clearly, the intermediate domains are responsible for isothermal ageing: they are at the origin of the observed decay of ε' (and C) represented by the coefficient Q. The very slow domains do not evolve at the plateau temperature; they only change the asymptotic behaviour of ε' in accordance with the sample thermal history and therefore they cause ergodicity breaking. The fast domains can instantaneously follow a (reasonable) temperature change. Their surface, together with the domain volume, provide the instantaneous variation ε' (and C) represented by the coefficient P. In such a scheme, based on the partition into the three types of domain, this coefficient is only weakly dependent on the thermal history. Our experiments cannot exclude such a weak dependence on the cooling rate.

Finally, the overall agreement of our results on KLT with the domain model supports the appropriateness of this simple description. In particular, it shows that a domain is correctly and sufficiently well described by the single parameter which characterizes its size. More precisely, the dielectric properties of a domain are related to the mean area calculated with the mean value of its radius. This shows that it is not necessary to introduce two or three lengths to describe the domain shape or to take into account some irregularities on the surface (then the standard deviation of the radius would not be negligible in comparison with its mean value). Since KLT and KTN crystals originate from the same $KTaO_3$ lattice, it is quite natural to compare them. A quantitative discussion of their differences (especially concerning return to disorder and memory) probably passes through a better understanding of the role of the SRF (due to Li^+ in KLT and Nb^{5+} in KTN) and through the evaluation of microscopic parameters such as barrier height and relaxation time.

References

[1] Lundgren L, Svedlindh P, Norblad P and Beckman O 1983 *Phys. Rev. Lett.* **51** 911
[2] Lefloch F, Hammann J, Ocio M and Vincent É 1992 *Europhys. Lett.* **18** 647
[3] For a review, see Vincent É, Hammann J, Ocio M, Bouchaud J-P and Cugliandolo L 1997 *Sitges Conference on Glassy Systems* ed M Rubi (Berlin: Springer)
[4] Struik L C E 1978 *Physical Ageing in Amorphous Polymers and Other Materials* (Amsterdam: Elsevier)
[5] Doussineau P, Levelut A and Ziolkiewicz S 1996 *Europhys. Lett.* **33** 391

[6] Albérici-Kious F, Doussineau P and Levelut A 1997 *J. Physique* I **7** 329
Doussineau P, de Lacerda-Arôso T and Levelut A *Eur. Phys. J.* submitted
[7] Palmer R G 1982 *Adv. Phys.* **31** 669
[8] Bouchaud J-P 1992 *J. Physique* I **2** 1705
[9] Albérici-Kious F, Bouchaud J-P, Cugliandolo L F, Doussineau P and Levelut A 1998 *Phys. Rev. Lett.* **81** 4987
[10] Doussineau P, de Lacerda-Arôso T and Levelut A 1999 *Europhys. Lett.* **46** 401
[11] Novotná V, Fousek J, Kroupa J and Hamano K 1991 *Solid State Commun.* **77** 821
[12] Jonason K, Vincent É, Hammann J, Bouchaud J P and Norblad P 1998 *Phys. Rev. Lett.* **81** 3243
[13] Bellon L, Ciliberto S and Laroche C 1999 *Preprint* cond-mat/9906162
[14] Vincent É, Dupuis V, Alba M, Hammann J and Bouchaud J P 1999 *Preprint* cond-mat/9908030 *Europhys. Lett.* submitted
[15] Jamet J P and Lederer P 1983 *J. Phys. Lett* **44** L-257
[16] Höchli U T, Knorr K and Loidl A 1990 *Adv. Phys.* **39** 405
[17] Vugmeister B E and Glinchuk M 1990 *Rev. Mod. Phys.* **62** 993
[18] Kleeman W 1993 *Int. J. Mod. Phys.* B **7** 2469
[19] van der Klink J J, Rytz D, Borsa F and Höchli U T 1983 *Phys. Rev.* B **27** 89